

Viewpoint Paper

Plastic deformation mechanism in nanotwinned metals: An insight from molecular dynamics and mechanistic modeling

Ting Zhu^{a,*} and Huajian Gao^{b,*}

^aWoodruff School of Mechanical Engineering, Georgia Institute of Technology, Atlanta, GA 30332, USA

^bSchool of Engineering, Brown University, Providence, RI 02912, USA

Available online 28 January 2012

Abstract—An overview is given of the deformation mechanisms in nanotwinned copper, as studied by recent molecular dynamics, dislocation mechanics and crystal plasticity modeling. We highlight the unique role of nanoscale twin lamellae in producing the hard and soft modes of dislocation glide, as well as how the coherent twin boundaries affect slip transfer, dislocation nucleation, twinning and detwinning. These twin boundary-mediated deformation mechanisms have been mechanistically linked to the mechanical properties of strength, ductility, strain hardening, activation volume, rate sensitivity, size-dependent strengthening and softening in nanotwinned metals. Finally, discussions are dedicated to identifying important unresolved issues for future research.
© 2012 Acta Materialia Inc. Published by Elsevier Ltd. All rights reserved.

Keywords: Twinning; Molecular dynamics; Modeling; Dislocation; Plastic deformation

1. Introduction

Ultrafine-grained copper (grain size $\sim 1 \mu\text{m}$) containing layered growth nanotwins (lamella thickness $\sim 20 \text{ nm}$) exhibit an unusual combination of ultrahigh yield strength ($\sim 1 \text{ GPa}$) and high ductility ($\sim 14\%$ elongation to failure) [1,2]. This unique nanotwinned metallic system has been the subject of intensive research in the past several years. It represents a novel class of nanostructured materials that opens up exciting possibilities of engineering the coherent internal boundaries to achieve unprecedented properties [3–5]. It is also an ideal model system where the high-level control of nanostructure processing and characterization facilitates a direct coupling between experiments and modeling [6,7]. Such coupled studies are crucial to advance the understanding of deformation mechanisms in nanostructured materials [8,9].

In this paper, a brief overview is provided of the deformation mechanisms revealed by recent modeling studies. Among different modeling approaches, molecular dynamics (MD) simulations have been performed to obtain an atomically resolved understanding of dislocation–twin boundary (TB) interactions [10–18]. Recently, massively parallel MD has been employed to study the strengthening and softening in polycrystalline nanotwin-

ned metals with more realistic three-dimensional microstructures and size scales [6,19]. To overcome the time scale limitation of MD, the atomistic reaction pathway was modeled to investigate the effects of temperature and strain rate on plastic yielding on the time scale of laboratory experiments [7]. Furthermore, the mechanistic modeling of dislocation mechanics and crystal plasticity facilitates a direct connection between macroscopic deformation behavior and the underlying dislocation mechanisms [20–26]. These modeling studies have underscored the unique role of coherent TBs in the deformation mechanisms of nanotwinned metals.

2. Size-strengthening is mediated by hard and soft modes of slip

In nanotwinned metals the high strength originates from the size-strengthening effect associated with nanoscale twin lamellae. This is consistent with the commonly recognized notion of “the smaller, the stronger” in nanocrystalline metals [27]. To appreciate such a twin-size strengthening effect, we recall that in conventional face-centered cubic (fcc) polycrystalline metals the plastic deformation is usually produced by dislocation glide on 12 equivalent $\{111\}\langle 110\rangle$ slip systems. It is well established that grain boundaries, which are generally incoherent, can impede the movements of dislocations. Continued plastic deformation requires the

* Corresponding authors. E-mail addresses: ting.zhu@me.gatech.edu; huajian_gao@brown.edu

applied load to achieve a critical level, so as to activate the dislocation sources and activities in neighboring grains. As a result, the grain size becomes a strength-controlling microstructural length scale. In nanocrystalline materials, dislocation glide is limited by the decreased grain size, which generally results in an increase in strength. Within nanosized grains, the $\{111\}\langle 110\rangle$ slip systems are still equivalent. However, the confined volume of nanograins tends to suppress the formation of trailing partials, thus promoting the activities of partial dislocations [28].

In contrast to nanocrystalline materials, nanotwinned fcc metals possess two characteristic microstructural length scales: the relatively large grain size, d , and the small twin thickness, λ . The former is typically on the micrometer scale, while the latter can be experimentally controlled in the range of a few to tens of nanometers [2]. A direct consequence of the two drastically different length scales is the creation of hard and soft modes of dislocation glide [21,22]. Consider, for example, the extended dislocations in the $\{111\}\langle 110\rangle$ slip systems, as represented by either of the double Thompson tetrahedra in Figure 1(a). Importantly, these $\{111\}\langle 110\rangle$ slip systems are no longer equivalent, owing to the presence of TBs. Depending on the orientations of the slip plane and the slip vector relative to the twin plane, they can be classified into three categories: (i) hard mode I (both the slip plane and Burgers vector are inclined to TBs), represented by the dislocation in blue in Figure 1(a); (ii) hard mode II (the slip plane is inclined to TBs, but the Burgers vector is parallel to TBs), represented by the dislocation in green; and (iii) soft mode (both the slip plane and Burgers vector are parallel to TBs), represented by the dislocation in orange. The slip resistances in both hard modes I and II are large due to the constraints of the small TB spacing λ on dislocation glide. In contrast, the slip resistance in the soft mode is much lower, because of less constraint as a result of the relatively large grain size d .

Activation of either the hard or soft mode of dislocation glide can be controlled by the loading orientation. Each slip mode, in turn, generates plastic shear or the equivalent tensile/compressive deformation in a specific orientation for accommodating the imposed displacements. Furthermore, different slip modes are usually associated with different dislocation sources. As schematically shown in Figure 1(a), hard mode I usually corresponds to the dislocations nucleated from the TB sources (e.g. ledges) or transmitted from the adjoining twin lamellae. Since the primary slip systems can be determined based on the largest resolved shear stress, a simple analysis of the Schmid factors indicates that hard mode I can be activated favorably by imposing tension/compression perpendicular to the twin plane. For hard mode II, dislocations usually nucleate near grain boundaries, traverse through the slender twin lamellae and stop near grain boundaries at the opposite side of the twin lamella. This hard mode of slip can be activated favorably by applying tension/compression parallel to the TB. In the extreme case when the maximum shear stress is oriented parallel to the twin plane, the soft mode of slip dominates, producing tension/compression at 45° to the twin plane.

As discussed earlier, the small microstructure size, i.e. the nanoscale TB spacing, tends to encourage the activities of partial dislocations in the $\{111\}\langle 112\rangle$ slip systems. In

particular, the glide of twinning partials on TBs mediates the TB migration, giving rise to the deformation-induced twinning or detwinning that leads to either hardening or softening behavior [6,17,29,30], as will be further discussed later. The studies of soft and hard modes of slip in terms of both extended and partial dislocations provide a useful basis for understanding the plastic responses of nanotwinned metals, particularly in the cases where the local load is already known or can be well controlled. Examples include columnar-grained thin film containing nanotwins [31–33], twinned nanowires and nanopillars [34,35], and transmission electron microscopy experiments of dislocation–twin interactions [17,36]. Finally, it should be noted that, in polycrystalline samples containing a large number of randomly oriented grains, deformation compatibility at grain boundaries usually requires the simultaneous operation of several slip systems. This is necessary to allow the grain to deform to shapes demanded by its neighbors. In such cases, the macroscopic plastic flow involves the operation of both the hard and soft modes of slip, as shown in Figure 1(b) and (c) [6]. While the nanometer-scale twin thickness appears to play a central role in strengthening [21–24], how the interplay of the two slip modes affects the apparent strength is not yet well understood.

3. Dislocation–twin boundary interactions

The coherent TBs in nanotwinned metals are not only responsible for their unique strengthening mechanisms by providing the hard and soft modes of slip, but also play an important role in rate sensitivity, activation volume, strain hardening and size softening [5]. To study these mechanistic effects, it is essential to understand the elementary processes of dislocation–TB interactions. Since the density of TBs increases with decreasing twin thickness, such interactions become increasingly frequent and thus more important in nanoscale twin lamellae.

As shown in Figure 1, TBs can oppose the expansion of dislocation loops for both hard mode I and II. To sustain plastic deformation, the obstructed dislocations may expand laterally within the slender twin lamellae, leaving behind long segments near TBs. Such dislocation segments tend to cut across the TB, transmitting into the adjoining twin lamellae. Alternatively, they may be absorbed into coherent TBs, where dislocations can easily glide to leave room for subsequent absorption. Another possibility is that the dislocations within TBs may desorb into the twin lamellae, forming lattice dislocations. These processes of dislocation absorption, desorption and direct transmission are generally referred to as slip transfer [37].

Atomistically detailed studies of slip transfer have been performed by MD [10–12]. The simulation results have revealed important differences between screw and non-screw dislocations. For a screw dislocation parallel to the intersection between the incoming and outgoing slip planes, its slip transfer does not leave a remnant dislocation component in the twin plane, as shown in Figure 2(a and b). However, the slip transfer of non-screw dislocations does, as shown in Figure 2(a and c). More importantly, the athermal shear stress of instantaneous slip transfer for a screw dislocation is estimated to be between 300 and 400 MPa [7,10,12], while that of a non-

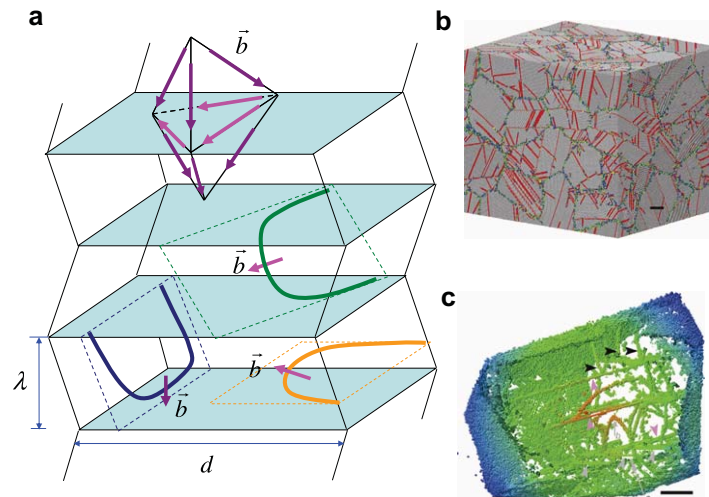


Figure 1. Twin-boundary-mediated dislocation activities in nanotwinned fcc metals. (a) Schematics of hard modes I (blue) and II (green) and soft mode (orange) of dislocation glide; the double Thompson tetrahedra indicate the $\{111\}(110)$ slip systems in the two adjoining lamellae. (b) Atomic configuration from a massively parallel MD simulation, showing the formation of a large number of dislocations during the plastic deformation of nanotwinned polycrystalline Cu [6]. (c) A magnified snapshot showing three-dimensional (3-D) dislocation structures; the dislocations intersect (black and grey arrows) or lie parallel to (purple arrows) the TBs [6]. The scale bars in (b and c) are 5 nm. (For interpretation of the references to colour in this figure legend, the reader is referred to the web version of this article.)

screw dislocation can be as high as 1 GPa [11]. Such a large discrepancy between the critical shear stresses of slip transfer seems to imply that the screw and non-screw dislocations play different roles in controlling the strength of ultrafine-grained nanotwinned Cu, but this issue has not been fully explored.

To understand the temperature effect on slip transfer, atomistic reaction pathway modeling was performed by using the nudged elastic band (NEB) method [7]. This approach does not suffer from the same time scale limitation as MD. From the NEB calculations, the minimum energy paths and associated activation energy barriers can be determined for dislocation absorption, desorption and transmission at the TB. Figure 2(b) shows an example of a NEB calculation on the absorption of a screw dislocation into a coherent TB. According to the transition state theory, at finite temperatures a reaction with a finite energy barrier would occur within a finite time with the aid of thermal fluctuations. At room temperature, slip transfer with an energy barrier of about 0.7 eV should occur frequently on the typical time scale of laboratory experiments (~ 1 ms). Note that increasing the stress can lower the energy barrier of the slip transfer. It follows that one can take the stress that gives an energy barrier of 0.7 eV as the critical load of the slip transfer at room temperature. For the slip transfer of a screw dislocation across TB, the critical shear stress at room temperature was estimated to be about 70% of the athermal critical stress [7]. A similar temperature effect is expected for non-screw dislocations.

The atomistic reaction pathway modeling also provided insights into the strain-rate effect, usually characterized in terms of activation volume and rate sensitivity. Nanotwinned Cu has been measured with reduced activation volume and increased rate sensitivity, and compared with its twin-free counterparts [21,38,39]. Computationally, one can determine the activation volume by calculating the energy barriers at different applied stresses, then taking the numerical derivative of

the energy barriers with respect to stress. The NEB calculations have shown that slip transfer at the TB gives characteristically small activation volumes, $10 \sim 20b^3$ (where b is the Burgers vector length) [7], consistent with experimental measurements [21]. Such small activation volumes imply that only a small group of atoms are involved during the thermal activation of slip transfer. This can be appreciated by examining the saddle-point atomic structure in a slip transfer reaction, as shown in Figure 2(b). The figure reveals essentially a cross-slipping process of local constriction of the stacking fault in the original slip plane and simultaneous bow-out in the cross-slipped plane. From the mechanics standpoint, the small activation volume, V^* , in nanotwinned Cu can be attributed to the fact that the material is subjected to an ultrahigh stress σ at the gigapascal level, so that the stress work σV^* associated with a small activation volume can lower the effective energy barrier to a level sufficient to initiate slip transfer at a TB within the time scale of laboratory experiments (seconds to minutes). In addition, a dislocation pile-up model has been developed to rationalize the twin size dependence of activation volumes in terms of relative importance of the intra- and inter-twin dislocation mechanisms [21,38,39].

Recent MD simulations [24,40] have also revealed an intrinsic capability of TBs to trap a high density of dislocations. In these simulations, a crack is introduced in front of a TB, as illustrated in Figure 3(a). When the sample is loaded, the crack serves as a “dislocation gun” that shoots out a massive number of dislocations toward the TB. As these dislocations impinge on the TB, they either remain in, slip across, or decompose into residual and transmission dislocations on the TB. In this way, the TB becomes decorated with a high density of dislocation debris, transforming into a dislocation wall, as illustrated in Figure 3(b and c). This dislocation wall blocks further dislocation motion, resulting in strain hardening [24], and becomes increasingly impenetrable to further slip transmission, rendering the TB more resistant to crack propagation [40].

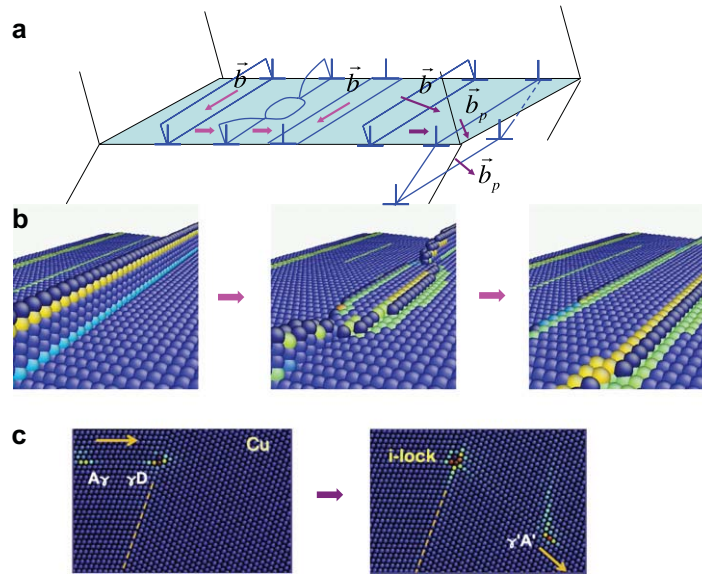


Figure 2. Atomistic modeling of dislocation–TB interactions. (a) Schematics of dislocation absorption and transmission at a TB. (b) The NEB result showing the atomistic pathway of dislocation absorption; the initial and final state is a straight screw dislocation consisting of the leading and trailing partials, while the saddle-point state (the middle image) involves a 3-D process of constriction and simultaneous bow-out of stacking faults [7]. (c) MD snapshots of slip transmission, showing an impinging non-screw dislocation decomposed into a transmitted partial dislocation and a dislocation lock at the TB [11].

Figure 3(d) indicates that there exists a boundary layer near the TB where dislocation densities are much higher than elsewhere. The dislocation wall is found to span about 6 nm across the TB, irrespective of the local dislocation density and the strain level, which is consistent with experimental observations and the twin-boundary-affected-zone model [21]. In situ tensile experiments inside a transmission electron microscope have demonstrated that dislocation-wall-strengthened TBs can strongly confine crack nucleation and resist crack propagation, leading to crack bridging by nanoscale twins [40].

4. Strain hardening and size softening

In addition to dislocation glide and slip transfer, coherent TBs can also critically affect dislocation nucleation, multiplication, twinning and detwinning, which underlie the unique strain-hardening and size-softening behavior of nanotwinned Cu. A high rate of strain hardening was measured during the initial stage of plastic deformation [41]. Such strain hardening behavior is highly desirable, as it serves to delay the onset of necking, thus promoting tensile ductility. In addition, the strongest size was revealed in nanotwinned Cu [2]. It was shown that the strength increases with decreasing twin thickness, reaching a maximum at about 15 nm, followed by a softening at smaller values.

To understand the TB-mediated strain hardening, we note that, in nanocrystalline materials, dislocation multiplication and accordingly strain hardening are severely limited by the confined space within the equiaxed nanograins. However, nanotwinned metals possess two drastically different microstructural length scales of grain size and twin thickness. While the nanometer-scale twin thickness appears to play a central role in strengthening, the micrometer-scale grain size can effectively facilitate

strain hardening. Within the slender twin lamellae, dislocations could multiply and accumulate in directions parallel to the TBs, forming tangles that subdivide the twin lamellae, thus leading to strain hardening [29]. Moreover, there exists significant stress concentration at the intersections between TBs and grain boundaries. These intersections can act as sources of dislocation nucleation. The dislocations, once nucleated, can easily glide on the coherent TBs. As discussed earlier, this soft mode of slip leads to the migration of TBs, causing twinning or detwinning. As those dislocations move away from the nucleation sites, space is created for subsequent dislocation nucleation. Figure 4(a) shows an MD snapshot at a point when a large number of dislocation loops have nucleated from the grain boundary–TB intersections [6]. Since the plastic deformation induced by the soft slip mode alone cannot easily be made compatible between adjoining grains, an alternative explanation for the observed high rate of strain hardening is that the incompatible plastic deformation is compensated for by elastic deformation, leading to a rapid build-up of back stresses in individual grains to resist further dislocation nucleation and propagation.

To understand the twin-size-dependent softening, we note that reducing the twin thickness in the grains can produce more intersections between grain boundaries and TBs, and thus more easy sources of dislocation nucleation. This can lead to the increased rate of dislocation nucleation under the same load, or equivalently the decreased flow stress for sustaining the same plastic strain rate. Such twin-size-mediated softening of strength has been qualitatively confirmed by MD simulations [6]. Furthermore, a theory has been developed by considering the kinetics of dislocation nucleation and available source density (i.e. the number of grain boundary–TB intersections) in such materials, so as to link the MD simulations with experiments. In this theory [6], the

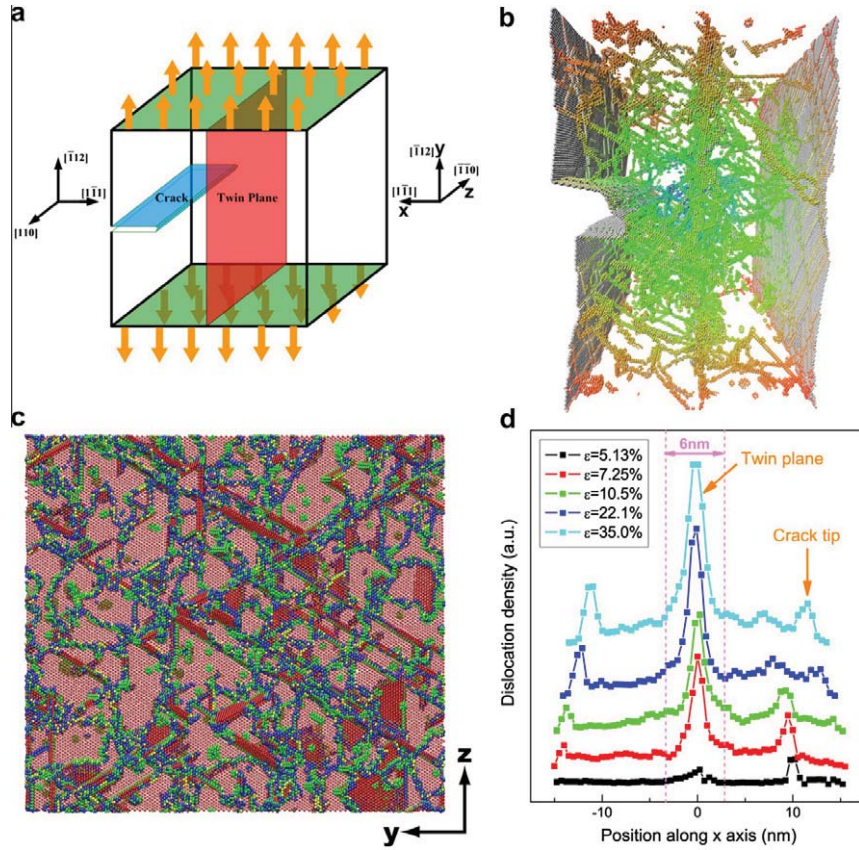


Figure 3. MD simulations of the twin-boundary-affected-zone (TBAZ) through the interaction between a pre-existing TB and a large number of dislocations generated from a crack tip [24]. (a) Schematic view of the simulation sample. (b) A snapshot of dislocation structures, showing that the TB has become a wall of high dislocation density which can harden the material by blocking further dislocation activities. (c) Patterns of dislocation structures remaining on the TB. (d) Dislocation density distribution near a twin plane, showing the characteristic thickness of the TBAZ to be around 6 nm.

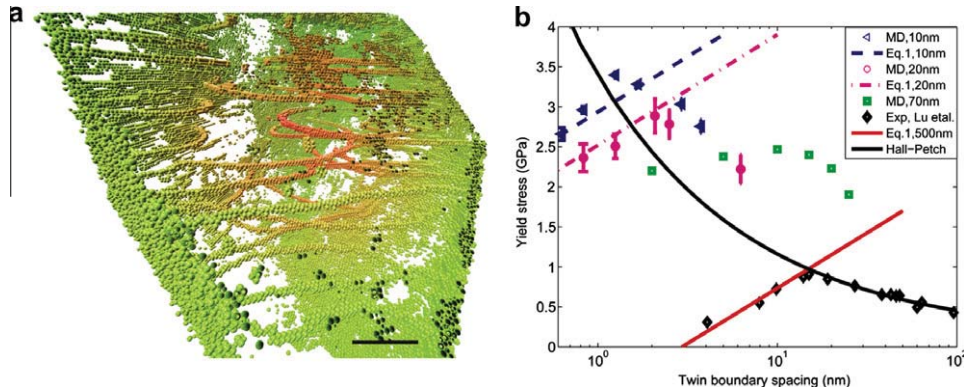


Figure 4. Twin-boundary-mediated softening in nanotwinned Cu [6]. (a) MD snapshot showing that a large number of dislocation loops nucleate from grain boundary–TB intersections (scale bar = 5 nm). (b) Comparison of experiment, MD and modeling prediction from Eq. (1) for the yield stress as a function of TB spacing at different grain sizes.

strength of the material depends on both TB spacing λ and grain size d ,

$$\sigma = \frac{\Delta U}{SV^*} - \left(\frac{k_B T}{SV^*} \right) \ln \left(\frac{d}{\lambda} \cdot \frac{v_D}{\dot{\epsilon}} \right) \quad (1)$$

where ΔU is the activation energy at zero stress, S is a factor representing local stress concentration and geometry, V^* is the activation volume, k_B is the Boltzmann constant, T is temperature, v_D is the Debye frequency

and $\dot{\epsilon}$ is the macroscopic strain rate. Figure 4(b) shows a comparison of the yield stress from the experimental data, the model predictions based on Eq. (1) and the MD simulation results [6]. Both simulations and the theory consistently show that TB spacing governs the softening in nanotwinned metals. Figure 4(b) also indicates that the onset of softening depends on the grain size: the smaller the grain size, the smaller the critical twin-boundary spacing and the higher the maximum strength of the material.

5. Prospects for future research

In summary, nanotwinned metals offer substantial potential for achieving superior properties by engineering the coherent internal interfaces. Molecular dynamics and mechanistic modeling have provided novel insights into the nanotwin-mediated deformation mechanisms. Among a vast list of potentially intriguing directions for future research, several areas present particularly pressing needs. For instance, how the interplay between the hard and soft modes of slip controls the deformation compatibility and consequently affects strength and ductility is not well understood. Similarly, going beyond the unit-process study, it is important to study how the macroscopic mechanical properties are governed by the interplay of different slip transfer modes at TBs. This study should involve various combinations of incoming and outgoing edge and screw dislocations, as well as the competing processes of twinning and detwinning that are particularly encouraged by the large number of intersections between TBs and grain boundaries. Combining in situ experiments with mechanistic modeling represents a promising approach to addressing these issues [17,42].

Most of the current studies have been focused on nanotwinned Cu. The potential of other types of nanotwinned metals remains largely unexplored [43,44]. Modeling studies of a variety of fcc metals have indicated that TB-mediated strength, ductility and twin stability can be critically influenced by stacking-fault-related properties, such as the stacking fault energy, unstable stacking and twinning energies [45,46]. Even for Cu, how to make bulk nanotwinned samples [47] and how to elucidate the mechanisms related to fracture, fatigue, damage tolerance and irradiation resistance are just beginning to be studied [48,49]. Figure 3 and associated discussions give an example of molecular dynamics modeling that provides insights into the crack-tip and TB interactions, while more systematic studies are needed in the future. Tackling these problems presents many challenges and opportunities for experimenters and modelers to work together to understand, control and optimize the remarkable properties of nanotwinned metals.

References

- [1] L. Lu, Y.F. Shen, X.H. Chen, L.H. Qian, K. Lu, *Science* 304 (2004) 422.
- [2] L. Lu, X. Chen, X. Huang, K. Lu, *Science* 323 (2009) 607.
- [3] S. Mahajan, D.E. Barry, B.L. Eyre, *Philosophical Magazine* 21 (1970) 43.
- [4] J.W. Christian, S. Mahajan, *Progress in Materials Science* 39 (1995) 1.
- [5] K. Lu, L. Lu, S. Suresh, *Science* 324 (2009) 349.
- [6] X.Y. Li, Y.J. Wei, L. Lu, K. Lu, H.J. Gao, *Nature* 464 (2010) 877.
- [7] T. Zhu, J. Li, A. Samanta, H.G. Kim, S. Suresh, *Proceedings of the National Academy of Sciences of the USA* 104 (2007) 3031.
- [8] M. Dao, L. Lu, R.J. Asaro, J.T.M. De Hosson, E. Ma, *Acta Materialia* 55 (2007) 4041.
- [9] T. Zhu, J. Li, *Progress in Materials Science* 55 (2010) 710.
- [10] Z.H. Jin, P. Gumbsch, E. Ma, K. Albe, K. Lu, H. Hahn, H. Gleiter, *Scripta Materialia* 54 (2006) 1163.
- [11] Z.H. Jin, P. Gumbsch, K. Albe, E. Ma, K. Lu, H. Gleiter, H. Hahn, *Acta Materialia* 56 (2008) 1126.
- [12] M. Chassagne, M. Legros, D. Rodney, *Acta Materialia* 59 (2011) 1456.
- [13] Z.M. Chen, Z.H. Jin, H.J. Gao, *Physical Review B* 75 (2007) 212104.
- [14] A.J. Cao, Y.G. Wei, *Journal of Applied Physics* 102 (2007) 083511.
- [15] L. Li, N.M. Ghoniem, *Physical Review B* 79 (2009) 075444.
- [16] I. Shabib, R.E. Miller, *Acta Materialia* 57 (2009) 4364.
- [17] J. Wang, N. Li, O. Anderoglu, X. Zhang, A. Misra, J.Y. Huang, J.P. Hirth, *Acta Materialia* 58 (2010) 2262.
- [18] H.F. Zhou, S.X. Qu, W. Yang, *Modelling and Simulation in Materials Science and Engineering* 18 (2010) 065002.
- [19] Z.X. Wu, Y.W. Zhang, D.J. Srolovitz, *Acta Materialia* 59 (2011) 6890.
- [20] R.J. Asaro, S. Suresh, *Acta Materialia* 53 (2005) 3369.
- [21] M. Dao, L. Lu, Y.F. Shen, S. Suresh, *Acta Materialia* 54 (2006) 5421.
- [22] A. Jerusalem, M. Dao, S. Suresh, R. Radovitzky, *Acta Materialia* 56 (2008) 4647.
- [23] P. Gu, M. Dao, R.J. Asaro, S. Suresh, *Acta Materialia* 59 (2011) 6861.
- [24] L.L. Zhu, H.H. Ruan, X.Y. Li, M. Dao, H.J. Gao, J. Lu, *Acta Materialia* 59 (2011) 5544.
- [25] Y.J. Wei, *Materials Science and Engineering A* 528 (2011) 1558.
- [26] Y.T. Zhu, X.L. Wu, X.Z. Liao, J. Narayan, L.J. Kecskes, S.N. Mathaudhu, *Acta Materialia* 59 (2011) 812.
- [27] S. Yip, *Nature* 391 (1998) 532.
- [28] H. Van Swygenhoven, P.M. Derlet, A.G. Froseth, *Nature Materials* 3 (2004) 399.
- [29] E. Ma, Y.M. Wang, Q.H. Lu, M.L. Sui, L. Lu, K. Lu, *Applied Physics Letters* 85 (2004) 4932.
- [30] Y.B. Wang, M.L. Sui, E. Ma, *Philosophical Magazine Letters* 87 (2007) 935.
- [31] X. Zhang, H. Wang, X.H. Chen, L. Lu, K. Lu, R.G. Hoagland, A. Misra, *Applied Physics Letters* 88 (2006) 173116.
- [32] A.M. Hodge, Y.M. Wang, T.W. Barbee, *Scripta Materialia* 59 (2008) 163.
- [33] Z.S. You, L. Lu, K. Lu, *Acta Materialia* 59 (2011) 6927.
- [34] C. Deng, F. Sansoz, *Nano Letters* 9 (2009) 1517.
- [35] D.C. Jang, C. Cai, J.R. Greer, *Nano Letters* 11 (2011) 1743.
- [36] Z.W. Shan, L. Lu, A.M. Minor, E.A. Stach, S.X. Mao, *JOM* 60 (2008) 71.
- [37] T.C. Lee, I.M. Robertson, H.K. Birnbaum, *Scripta Metallurgica* 23 (1989) 799.
- [38] L. Lu, M. Dao, T. Zhu, J. Li, *Scripta Materialia* 60 (2009) 1062.
- [39] L. Lu, T. Zhu, Y.F. Shen, M. Dao, K. Lu, S. Suresh, *Acta Materialia* 57 (2009) 5163.
- [40] S. Kim, X. Li, H. Gao, S. Kumar, *Acta Materialia* 60 (2012), doi:10.1016/j.actamat.2012.02.002.
- [41] X.H. Chen, L. Lu, *Scripta Materialia* 57 (2007) 133.
- [42] S. Kumar, X.Y. Li, A. Haque, H.J. Gao, *Nano Letters* 11 (2011) 2510.
- [43] H. Idrissi, B.J. Wang, M.S. Colla, J.P. Raskin, D. Schryvers, T. Pardoen, *Advanced Materials* 23 (2011) 2119.
- [44] D. Bufford, H. Wang, X. Zhang, *Acta Materialia* 59 (2011) 93.
- [45] Y. Kulkarni, R.J. Asaro, *Acta Materialia* 57 (2009) 4835.
- [46] Z.H. Jin, S.T. Dunham, H. Gleiter, H. Hahn, P. Gumbsch, *Scripta Materialia* 64 (2011) 605.
- [47] Y.S. Li, N.R. Tao, K. Lu, *Acta Materialia* 56 (2008) 230.
- [48] A. Singh, L. Tang, M. Dao, L. Lu, S. Suresh, *Acta Materialia* 59 (2011) 2437.
- [49] C.J. Shute, B.D. Myers, S. Xie, S.Y. Li, T.W. Barbee, A.M. Hodge, J.R. Weertman, *Acta Materialia* 59 (2011) 4569.